ISSN : 0974 - 7443 Volume 10 Issue 6
CHEMICAL TECHNOLOGY
An Indian Journal
Full Paper
CTAIJ 10(6) 2015 [276-294]

Characterization of NiMoS and CoMoS nano particle supported TiO_2 -Al_2O_3 catalysts and their HDS performance in single and dual catalytic bed system

A.H.Samia*, S.M.Mohsen, A.S.El-sayed
Egyptian petroleum research institute (EGYPT)

ABSTRACT

Synthesis, characterization and catalytic evaluation of NiMo and CoMo supported on titania-modified alumina where carried out. For the synthesis of supported NiMo and CoMo catalysts, a molybdenum precursor acidic solution and aqueous nickel(cobalt) nitrate solution was used. The morphological as well as microstructural features of the prepared samples were analyzed by X-ray diffraction (XRD), Fourier transform infrared (FTIR) Transmission electron microscope (TEM) and temperature programmed reduction (TPR). Textural properties of supports and catalysts were also characterized by nitrogen physic-sorption. The hydrodesulforization(HDS) process was performed in a fixed bed down flow reactor at varying operating conditions,temperature(320-400 °C), LHSV (0.5-4 h^{-1}), H_2/ oil ratio of 450v./v.,and 6MPa operating pressure. Each catalyst was evaluated separately**.** The most active tow catalysts were tested in dual layer catalytic bed system to achieve the sulfur level less than 15 ppm. TPR spectra of the Co and Ni promoted catalyst showed that Ni promotes the easy reduction of Mo species compared to Co. TEM analysis show how the nature of the promoter as well as the support composition affected the morphology of the active MoS_2 phase and influenced its catalytic behavior. The experimental results show that The HDS efficiency reaches a maximum at NiMo/ TiO_2 -Al_2O_3 catalysts with Ti content of 15%, which is consistent with the higher reducibility of TiO_{2-} Al_2O_3 support and the higher CUS proportion. NiMo catalyst was found to be superior to CoMo catalyst for gas oil HDS. The dual catalytic bed system under respective conditions can be a logical approach to achieve the sulfur level lower than 15 ppm at acceptable reaction conditions.

KEYWORDS

Nano particle;
Synthesis;
Characterization single and dual catalytic bed;
HDS;
Gas oil.

INTRODUCTION

Industrial development and expanding transportation needs have increased environmental pollution; thus, stricter standards for gasoline and diesel fuel have been implemented, including decreased S content limits. To meet these limits, research has focused on catalysts and processes for desulfurization of gas oil. To achieve S levels of less than 10ppm for gas oil[1,2]. Deep HDS has been an issue in the desulfurization of refractory S species such as 4,6-dimethyldibenzothiophene (4,6-DMDBT), as well as the rapid

HDS of reactive S species.. The former issue can be resolved by the hydrogenation of a phenyl group in alkyldibenzothiophene (DBT) or by shifting the methyl groups in 4,6- DMDBT before HDS[3,4], whereas the latter issue can be solved by the rapid HDS of reactive sulfur species, allowing more time for the deep HDS of refractory S species, which tends to be slow. However, the most effective catalysts for solving these two issues are not always same. Thus, dual catalytic beds have been proposed for the rapid HDS of reactive S species and the deep HDS of refractory S species at low temperatures[5]. Attending this demand, many efforts are aimed to design new hydrotreating catalysts,highly active and selective for HDS of the refractory polyaromatic sulfur compounds[6–8]. It is known that the active phases of the HDS catalysts are the MoS_2 or WS_2 nano- particles promoted by cobalt or nickel atoms, deposited on high specific surface area supports. To modify the efficiency of such complex catalytic systems, different approaches have been tried, for example, the use of novel supports (oxide supports with ordered pore structure, nanostructured materials, etc.) and of novel active phases (noble metals, transition metal phosphides, etc.) or the search for new promoters and additives for the conventional HDS catalysts[9–16]. Among these options, development of novel supports seems to be an interesting and practical option because the support's nature and characteristics play an important role in the catalytic activity. It is well-documented that the support can influence reducibility and sulfidability, structure and dispersion of the deposited metal oxides, as well as the morphology of the sulfide active phases[17]. In the present study, NiMoS/ CoMoS catalysts were prepared and examined to evaluate the HDS of straight-run gas oil (SRGO) using single and dual catalytic beds. In addition the catalysts were characterized by BET, X-ray diffraction (XRD), FTIR,TEM and TPR to discuss the influence on their catalytic activities.

EXPERIMENTAL

Support preparation

Preparation of titania-alumina (Ti(x%)-Al)

Binary oxides supports were prepared by homogeneous delayed precipitation method from aqueous solutions of 0.1M $TiCl_4$ (Sigma-Aldrich) and 0.1M $AlCl_3$ (Aldrich), using aqueous NH_4OH solution (1:1) as a precipitating agent and controlling the pH at ≈ 8.5 under stirring (800 rpm.). The stirring was kept continuous for 4h to allow the complete mixing of the precipitate which was then filtered, washed and, dried at room temperature and subsequently at 120°C for 12h. The support was finally calcined at 550 °C for 6h.. By altering the relative amount of Ti Cl_4. and $AlCl_3$,a desired binary oxide could be obtained[18]. The supports examined in the present study are labeled (Ti(x%)-Al), x being the wt% of TiO_2 (Ti), Al represents Al_2O_3.

Preparation of alumina (Al)

The alumina support (Al) was prepared by the same method as (Ti(x%)-Al) without adding $TiCl_4$.

Preparation of titania (Ti)

For the preparation, analytical grade HCl (ca.37wt%, Merk) was used. $TiCl_4$ (>99%) precursor was supplied by Sigma-Aldrich and was stored at -15 °C in a refrigerator, to minimize fuming, which is observed when $TiCl_4$ reacts with airborne moisture. During the preparation, the $TiCl_4$ solution(0.1M) was slowly added to a well stirred vessel containing 200 ml of 0.1M HCl solution. The reaction mixture was kept in an ice-water bath, and was vigorously stirred during the drop wise (ca.0.5ml min^{-1}) addition of the calculated amount of $TiCl_4$ solution. At the place of dropping a yellowish precipitate was formed, which then instantaneously dissolved. At this point of preparation, all the systems in the concentration range investigated were transparent and free of any precipitate. The TiO_2 support was prepared by the alternate addition of the $TiCl_4$-HCl solution (20ml) and aqueous ammonia solution (30 ml) under vigorous stirring for 24h at room temperature. A white precipitate of hydrous TiO_2 was formed[19]. The sample was dried and calcined as mentioned before.

Catalyst preparation

The NiMo /or CoMo catalysts were prepared using incipient wetness sequential impregnation. First the molybdenum impregnation onto the supports was carried out using an aqueous solution of ammonium heptamolybdate (99.8%, Aldrich), and 6% of

Full Paper

TABLE 1 : Textural properties of supports and catalysts

Sample composition	Support			Catalyst [a]		
	Surface area, m^2 g^{-1}	Pore volume, ml g^{-1}	Average[b] pore diameter, nm	Surface area, m^2g^{-1}	Pore volume, ml g^{-1}	Average[b] pore diameter, nm
Al_2O_3	247	0.34	5.5	195.4	0.29	5.94
TiO_2	72	0.24	13.33	56	0.18	12.86
Ti(15%)-Al[a]	204	0.32	6.27	176	0.28	6.36
Ti(15%)-Al[c]	204	0.32	6.27	180	0.29	6.44
Ti(50%)-Al[a]	186	0.3	6.45	154	0.26	6.75

[a]:The active metal oxide MoO_3=10wt% and the promoter NiO=3.0 wt%, [b]: Average pore diameter= 4(Pore volume) X10^3 / Surface area c:The active metal oxide MoO_3=10wt% and the promoter CoO = 3.0 wt%.

TABLE 2 : Physico-chemical Properties of Gas Oil Feedstock

Characteristic	Value	Method
Specific gravity, 60/60 ºF	0.8340	ASTM D 289-65
Refractive index, 20 ºC	1.46417	ASTM D 1218-92
Component analysis, %		Silica-gel column
Total saturates	74	
Mono aromatics	14	
Di aromatics	8	
Poly aromatics	4	
Total aromatics	26	
Total sulfur, content, wt %	0.76	ASTM D 294-90 (x-ray fluorescence)
ASTM distillation(vol.%, ºC)		ASTM D 2887
IBP	190	
50%	320	
EP	360	

hydrogen peroxide, the latter was to increase the heptamolybdate solubility. The pH was adjusted to 2 by adding HNO_3 to avoid any precipitation of molybdenum compounds. The resulting solids were dried at 120°C[20,21]. Then the nickel/ or cobalt was incorporated by impregnation with an aqueous solution of nickel nitrate or cobalt nitrate, dried at 120°C for 6h and calcined at 550°C for 4h. The nomenclature and nominal composition of the prepared samples are presented in TABLE 1.

Supports and catalysts characterization

Surface area and pore volumes of the support and catalyst materials were determined from nitrogen adsorption-desorption isotherms measured at -196 °C from the linear BET plots using Quantachrome Nova 3200 instrument (USA). The measurements were performed on the oxide form of the sample. Before carrying out the measurement each sample was degassed under a reduced pressure of 10^{-5} torr at 150°C for 2h. The Infrared (IR) spectra were recorded on a ATI Mattson Genesis series (KBr disc method) apparatus, Model 960 M009 series, for characterization of support materials and catalysts. The final spectra were taken after 64 scans with 2 cm^{-1} resolution.. X-ray powder diffraction (XRD) patterns have been recorded on a Brucker AXS-D8 Advance (Germany) by using nickel-filtered copper radiation (λ =1.5405Å) at 60kv and 25mA with scanning speed of 8° in 20 min^{-1} over diffraction angle range. Transmission electron microscopic (TEM) analysis of the sulfided catalysts was carried out by using Zeiss (West Germany)TEM. Hydrogen temperature-programmed: reduction (H_2-TPR) experiments for precursor catalysts were carried out from room temperature to 1000 °C, with a flow of 10% H_2/N_2 (85ml min^{-1}) and a heating rate of 10°C min^{-1} using Chembet-3000 analyzer.

Catalytic activity measurement

The GO feedstock used in this investigation was kindly provided by Cairo Petroleum Refining Company. Its physicochemical characteristics are given in TABLE 2.

Our investigation was carried out in a down-flow micro-activity high presure unit. The unit consists mainly of an isothermal fixed bed 304 stainless steel tubular reactor having 13.1mm internal diameter, 19 mm external diameter and 505 mm long. the reactor was heated in an electric furnace. The reactor, furnace, radical emission type, has two heating zones independently controlled for an improved temperature profile. First. The catalyst bed was first sulfided with 2% dimethyldisulfide (DMDS)-cyclohexane mixture which was passed through the catalyst bet at the following conditions: hydrogen flow rate 0.5 ml/min, feed flow rate 0.5 ml/min and 4 LHSV h^{-1}. Sulfidation was performed at two different temperatures, the first sulfidation was done at 260 °C for 3h, and the second was performed at 360 °C for 3h[22-24]. The reaction conditions for all HDS processes were: reaction temperature, 325-400 °C, LHSV, 0.5-4h^{-1}, operating pressure, 6.0 MPa and H_2/ oil ratio of 450v./v. In all tests, the liquid product were analyzed according to ASTM standard methods as shown in TABLE 2. The catalyst performance tests were carried out in two systems:

Single stage operation, where each catalyst was tested in a single operation.

Dual bed system, where CoMo/Ti(15%)-Al and NiMo/Ti(15%)-Al in dual layer operation. The ratio of the catalyst types is 1/1.

RESULTS AND DISSCUSION

Catalyst characterization

The BET specific surface areas, total pore volumes and average pore diameters of pure alumina, titania, and their mixed oxides as well as for NiMo (CoMo) loaded catalysts are given in TABLE 1. The surface areas of alumina and titania were found to be 247 and 72 m^2g^1, respectively. Here it appears obviously the large surface area of the alumina (247 m^2g^{-1}) which is much larger than that prepared by most advanced methods such as spray pyrolysis method[25] reflecting how the method of preparation can improve the physical properties of the catalyst and so its catalytic activity, beside it reflects that we was successful to prepare supports with good characters by simple and economic method which we call simple idea my make a difference. Titania also has a good surface area (72 m^2g^{-1}), since by many other methods titania surface area doesn't exceed 50 m^2 g^{-1}[26] From TABLE 1, it can be seen that the specific surface areas of the mixed oxide supports decrease with the increase of TiO_2 loading, the minimal specific surface area reaches 186 m^2g^{-1} where the TiO_2 loading is 50wt%, this is a logic since titania has a very low surface area than alumina Hence we must choose the proper amount of titania that gives us the desired properties without sharp decrease in the surface area of the binary oxide support. From TABLE 1, it appears that, the introduction of titania with proper proportion to alumina (15%) exhibited textural properties similar to alumina and can keep the pore volumes and average pore sizes of composite supports at high levels, which would facilitate the adsorption and diffusion of the large molecule including refractory compounds such as dibenzothiophenes (DBTs) in gas oil. The surface areas of catalysts having 10wt% MoO_3 and 3wt% NiO(CoO) supported on the prepared oxides also show similar behavior, where the catalysts loaded on alumina have a large surface areas than those supported on titania, and those supported on Ti(15%)-Al are large than those supported on Ti-(50%)-Al. But, for all supports, with the addition of NiMo(CoMo) on the oxide supports a substantial decrease of surface area of the catalysts was observed, since the NiMo(CoMo) particles by the impregnation process may be introduced into the pores so blocking the pores and hinder the N_2 adsorption.

FT-IR analysis was utilized to determine the possible structural changes taking place in the supports and catalysts in the region 4000-400 cm^{-1}. Figures 1-3 show the spectra for the pure alumina, titania, mixed oxide supports Ti(50%)-Al and Ti(15%)-Al together with the spectra of the NiMoO (CoMoO) and NiMoS (CoMoS) containing catalysts after thermal and sulfiding treatment,respectively.. Figure 1a shows that the pure γ-Al_2O_3 structure was consid-

Full Paper

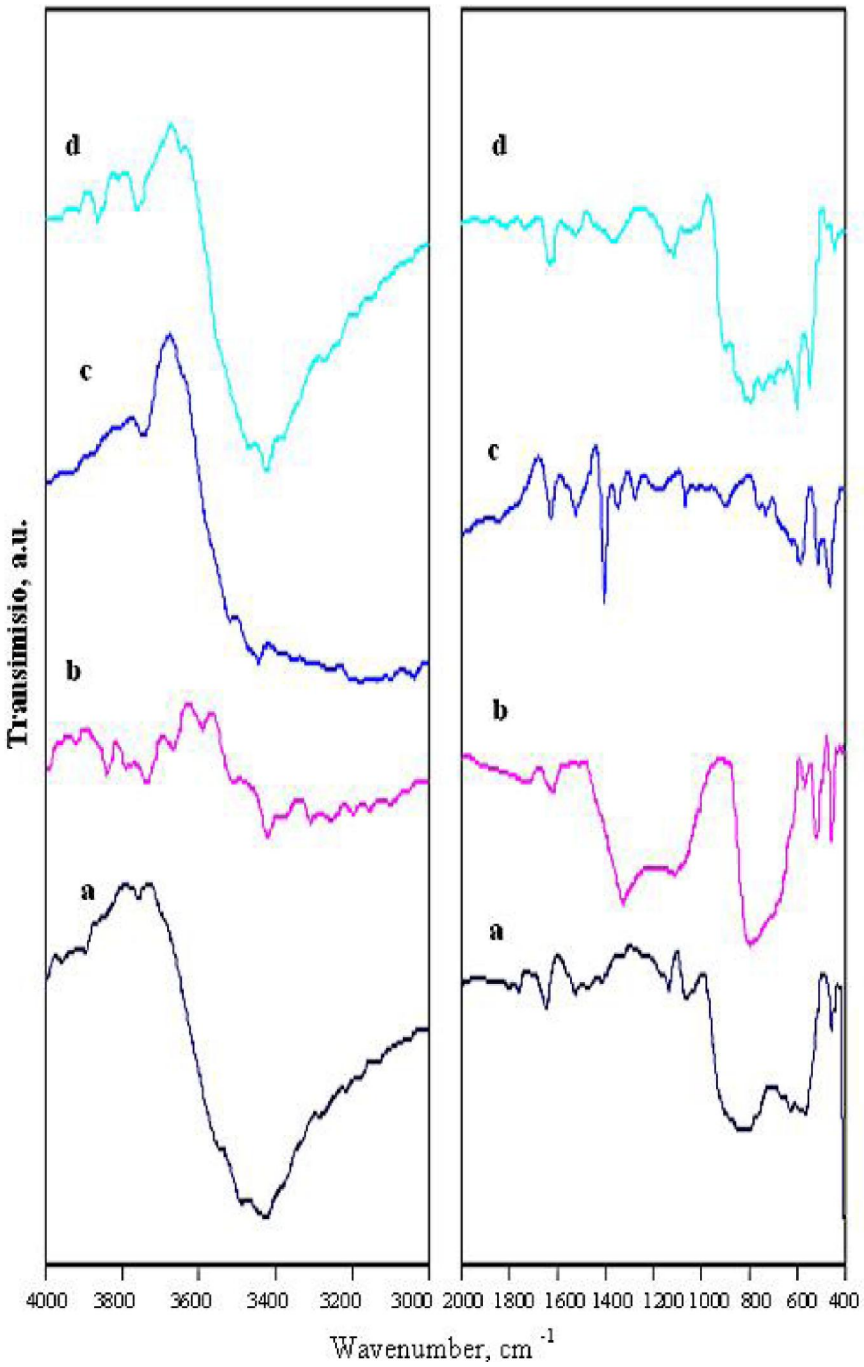

Figure 1 : FTIR spectra of supports: Al_2O_3 (a), TiO_2 (b), Ti(50%)- Al (c),A Ti(15%)-Al (d)

ered as hydrogen spinel and a broad absorption in the region 1100-400 cm^{-1}, which is the typical absorption band of γ-Al_2O_3[27]. The low frequency areas (500-600 cm^{-1}) should be dominated by the stretching vibration band of AlO_6 octahydra. The high-frequency areas 680-900 cm^{-1} can be associated with the stretching vibration band of AlO_4 tetrahedra. Beside, the pure alumina exhibited a new absorption band at 1406 cm^{-1}, which can be assigned to the longitudinal acoustical mode vibration of the nano- γ-Al_2O_3[28]. Several bands appeared in the external OH stretching region 4000-3000 cm^{-1} beside a new band appeared at 3900 cm^{-1}. A shoulder band appeared at 3790 cm^{-1} related to the terminal OH over one tetrahedrally coordinated aluminum ion in vacant environment, while the third feature at 3770 cm^{-1} appears as poorly resolved but very reproducible shoulder. This latter feature is of interest

here,that have been identified as arising from the type 1-a hydroxyl groups,i.e., those hydroxyl groups band to tetrahydrally coordinated aluminum atoms near a cation vacancy. Band appeared at 3735 cm^{-1} related to terminal OH over one octahedrally coordinated Al ion[29]. Broad intense bands between 3600 and 3300 cm^{-1} due to the OH stretching mode of layer hydroxyl groups and of interlayer water molecules. The extreme broadness of the OH band may be owed to the presence of the hydrogen bonding[30]. Figure 1b shows the strong absorption bands for pure titania in the region 400-600 cm^{-1}, which corresponds to the characteristic vibration of TiO_2 stretching and a broad band in the region 600-900 cm^{-1} and a band at 1064 cm^{-1}[31], new pronounced band appears at 1327 cm^{-1} which can be assigned to nano-structural TiO_2. Intense bands between 3500 and 3000 cm^{-1} due to the OH stretching mode of hydroxyl groups and water molecules. In addition, hydroxyl group bands related to TiO_2 appeared in the region 4000-3500 cm^{-1} (Figure1b). Figure1c, d shows the bands assigned to Ti(50%)-Al and Ti (15%) -Al binary oxide supports. The bands of TiO_2 in the Ti(15%)-Al support show the overlap with Al_2O_3 (Fig 1d). As titania content increase, the intensity of the TiO_2 bands increase (Figure 1c) assigned to the presence of TiO_2 on the external surface of Al_2O_3 in accordance to XRD (Figure4c). In other words, it is evident in the peak area of AlO_6 octahedra enlarges with the increasing TiO_2 content. These results indicate that, a significantly wide peak at 400- 600 $cm^{-1,}$ which corresponds to the characteristic vibration of Ti-O stretching covered the stretching vibration band of AlO_6 octahedra at 565 $cm^{-1,}$ which also shows that TiO_2 wraps the outside surface of γ-Al_2O_3. It is clear that, the peak intensity of AlO_4 tetrahedra weakens significantly as the TiO_2 content increases. These results show that the presence of TiO_2 decreases the amount of four-complexing Al^{+3} ions on the surface of γ-Al_2O_3 which are the active sites of the strong interaction between the metallic components and γ-Al_2O_3 support. In addition, other new hydroxyl group bands appeared.

Figure 2 shows the spectra of NiMoO and CoMoO containing catalysts. With the addition of 10 wt% MoO_3 and 3wt % NiO to Al_2O_3, the intensities of pure alumina bands at 444, 557 and 1050 cm^{-1} decrease and a new bands appeared at 583 and 826 cm^{-1} (Figure 2a) characteristic to MoO_2[32]. Concentrating on the isolated OH bands, the band at 3735 cm^{-1} shifted to 3745 cm^{-1} and strong attenuation of the higher frequency OH bands appear[33]. Figure 2b shows the broadening of the bands at 800-415 cm^{-1} and the shift of the band at 1327 to 1031 cm^{-1} due to the interaction between Ni, Mo oxides and titania. New bands appeared at 583 and 656 cm^{-1} attributed to the vibration of Mo=0 band of polymerized molybdate species interacting with the support[34]. The bands at 869, 966 and 1059 cm^{-1} can be assigned to Mo-O-Mo bending vibration (Figure 2b). On comparing the bands 893-464 cm^{-1}(Figure 2c) with those representing the IR of the original support (Figure1c), the same absorbance bands have appeared, the broadening of these bands, may be due to the combination of Ni and Mo oxides with the Ti(50%)-Al support. Octahedral coordinated MoO_6^{-6} is observed at 917 and 1120cm^{-1} (Figure 2c). Figure 2d shows the presence of octahedral coordinated MoO_6^{-6} at 982 cm^{-1}. There is no characteristic band of MoO_3 in Figure 2e, implying that, MoO_3 phases are highly dispersed on the composite supports due to the surface interaction between Co and Mo, which is consistent with the results of XRD. The modification of the alumina surface with titania (composite support) can weaken the interaction between γ -Al_2O_3 and Mo active phases and thus decrease the amount of four-complexing Al^{+3} ions, consequently improving the HDS activity of the catalyst[35]. All IR spectrum show the disappearance of the bands associated to NiO(CoO) indicating the interaction between NiO (CoO) and support[31]. All spectrum show the appearance of new bands may be related to:

Polysulfide compounds formed during the process of sulfiding[36].

b)The formation of Ni-Mo-S(Co-Mo-S) phase, resulted from either:

- The sulfiding of Ni-Mo-O(Co-Mo-O)[precursors of Ni-Mo-S (Co-Mo-S)], which has been formed from interaction of Ni (Co) and Mo oxides at the support surface[37].
- Localization of the NiS (CoS) on the MoS_2 edges[38].

Full Paper

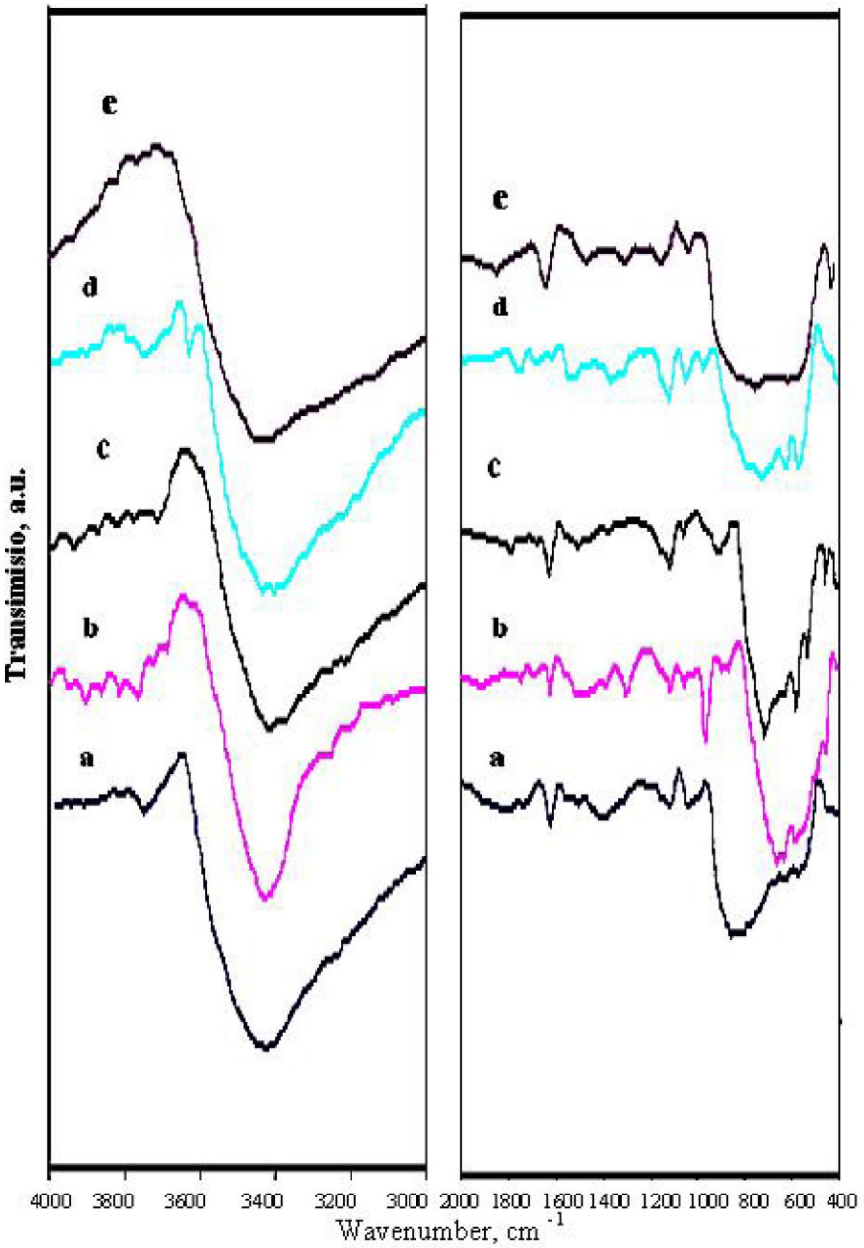

Figure 2 : FTIR spectra of NiMo supported on Al_2O_3(a), TiO_2 (b), Ti(50%)-Al(c), Ti(15%)-Al(d), and CoMo supported on Ti(15%)-Al(e)

Figure 2f shows new intensive bands appeared in the region 2000-464 cm^{-1} and 4000-3000 cm^{-1} which are an indication of the presence of sulfided titania particles. Figures 2, 3 clearly show that calcined catalysts consist of closely mixed MoO_2 and highly dispersed NiO(CoO) on the supports. Sulfidation converts these oxides into MoS_2 and Ni sulfide (Co_9S_8). MoS_2 crystals are the source of S-vacancies which are the HDS active centers known to be coordinatively unsaturated sites[35].

Figure 4-6 show the XRD patterns for pure alumina, titania and binary oxide supports, respectively, together with the NiMoO (CoMoO) and NiMoS(CoMoS) containing catalysts. Upon calcination, diffractogram in Figure4a exhibited some of broad peaks detected at 2θ, 37.28°, 45.7° and 66.37°, which were typical reflecting poorly crystalline γ-alumina phase, new diffraction peaks appear at 2 θ of 31.37° and 61.0°, can be assigned to the nano- γ- Al_2O_3 phase(JCPDS Card No.29-0063)[40]. The XRD patterns of pure titania support indicated the characteristic peaks of 100% anatase

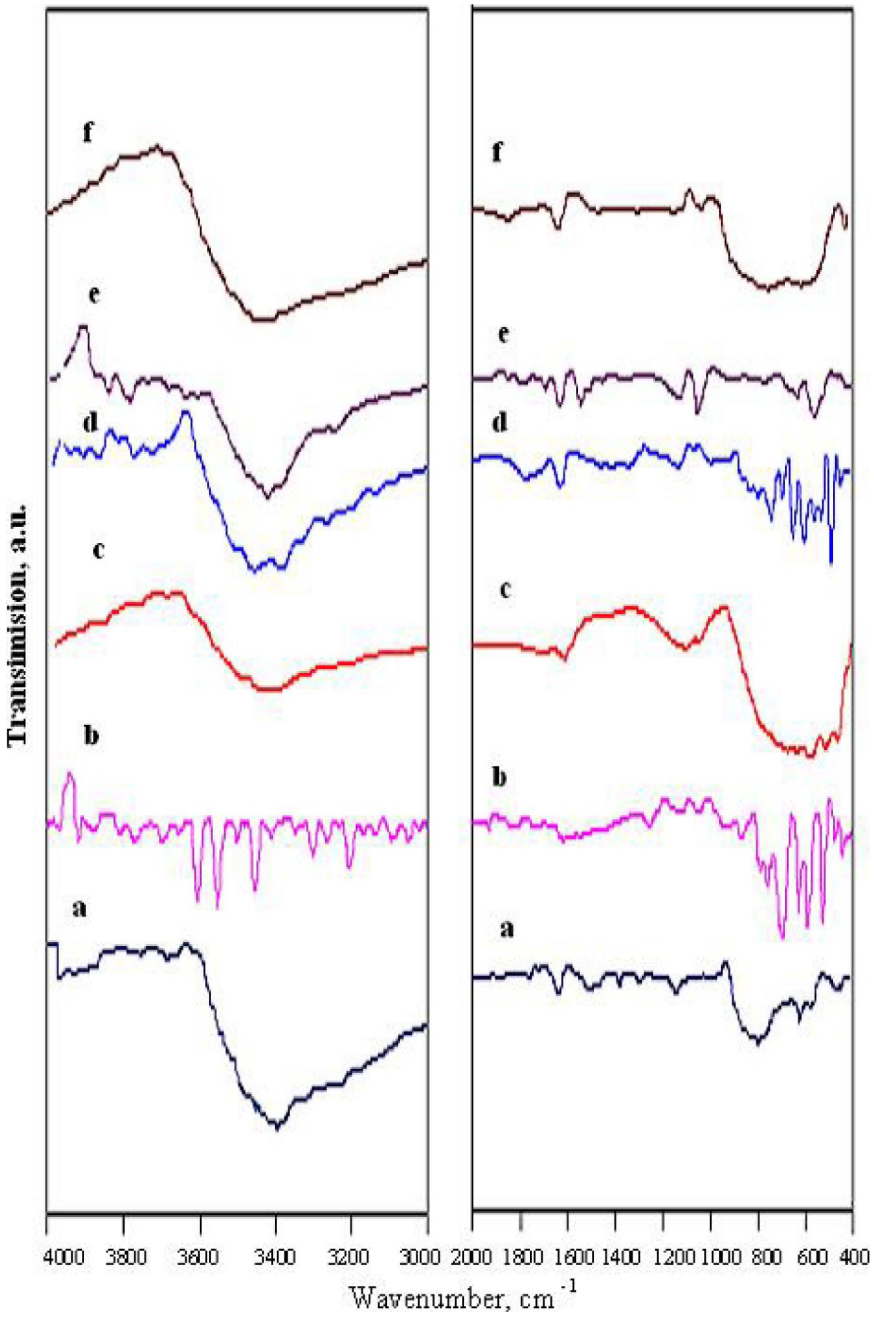

Figure 3 : FTIR spectra of NiMoS supported on Al_2O_3(a), TiO_2(b), Ti(50%)-Al(c), Ti(15%)-Al(d), CoMoS Supported on Ti(15%)-Al(e), and Sulfided TiO_2 support(f)

as evidenced by the sharp lines at 2θ of 25.28°(major), 36.98°, 37.83°,38.57°,48.06°, 53.96°, 55.14°, 62.74°, 68.84°, 70.28° and 74.91°(Figure4b)[41]. Figure4 c, d shows the XRD patterns of binary oxide supports; Ti(50%)-Al and Ti(15%)- Al. At 15% TiO_2, the peaks of anatase can be observed at 2 θ of 25.28°, 53.96 ° and 62.74°(Figure4d). At 50 wt% TiO_2 the peaks of γ -Al_2O_3 at the 2θ of 45.7 and 66.37º appear (Figure 4c), all typical peaks of anatase TiO_2 are present, indicating that, the clusters of accumulated TiO_2 becoming larger[42]. We also checked NiMo(CoMo) oxides and sulfide phases by XRD (Figures 5,6),but no major crystalline phase was detected according to the standard data (PDF-IDD) files[40], although the percentage of Ni(Co) is 3% and that of Mo is 10%. This is probably due to the formation of an amorphous phase containing Ni, Mo, O and S[43] as shown by TEM(Figure 7 a, d, e),

Full Paper

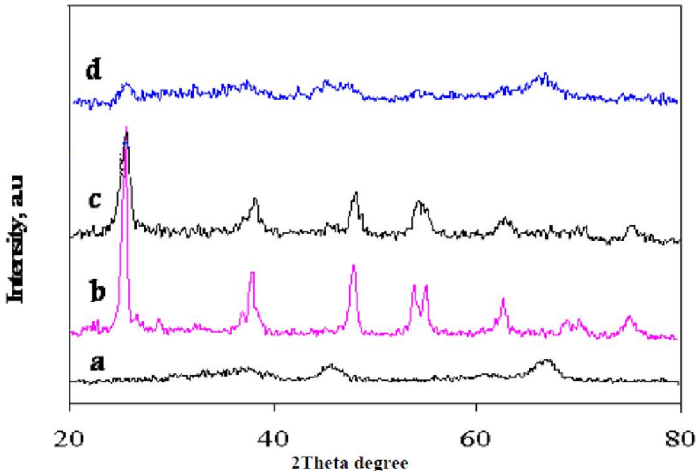

Figure 4 : X-ray diffractions of: Al_2O_3 (a), TiO_2 (b), Ti(50%)-Al (c) and Ti(15%)-Al (d)

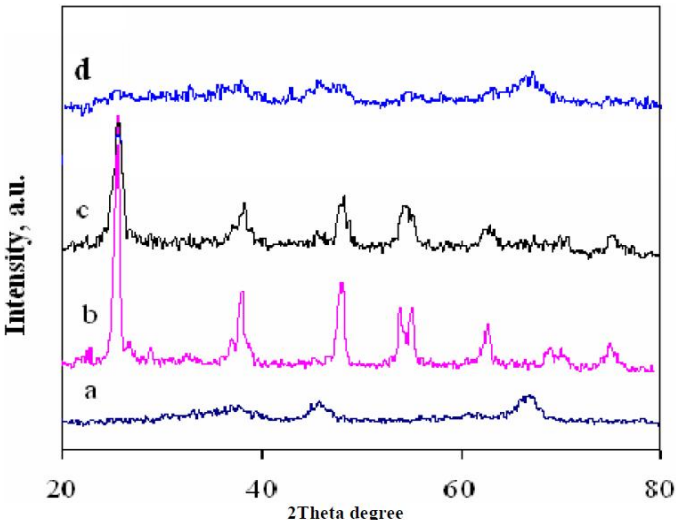

Figure 5 : X-ray diffractions of NiMo supported on: Al_2O_3 (a), TiO_2 (b), Ti(50%)-Al, and Ti(15%)-Al (d)

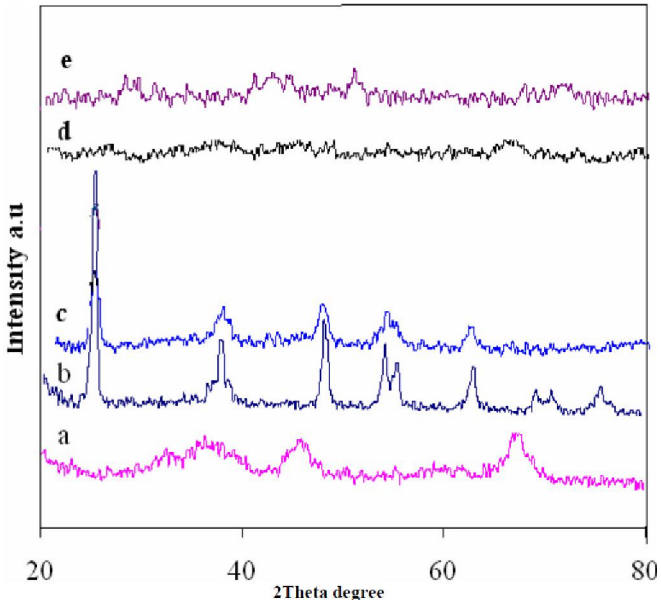

Figure 6 : X-ray diffractions of NiMoS supported on Al_2O_3 (a), TiO_2 (b), Ti(50%)-Al(c), Ti(15%)-Al (d), and CoMoS supported on Ti(15%)-Al(e)

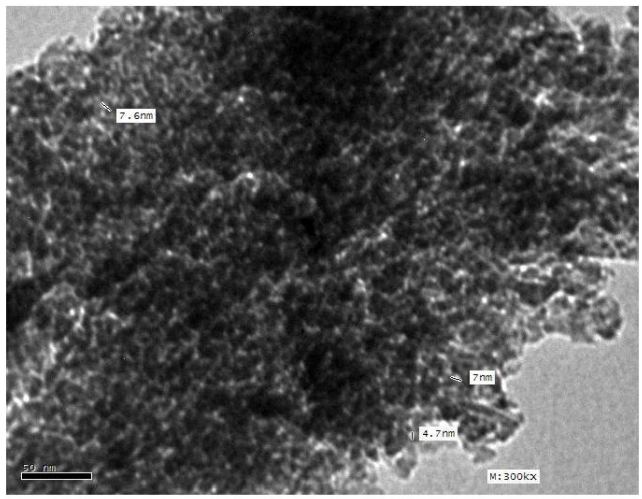

(a)

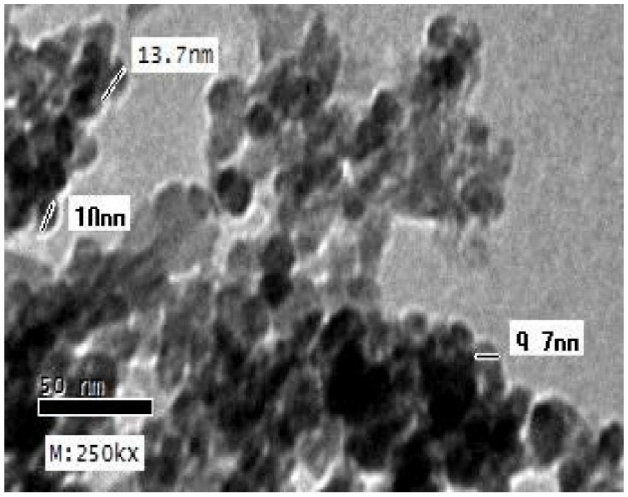

(c)

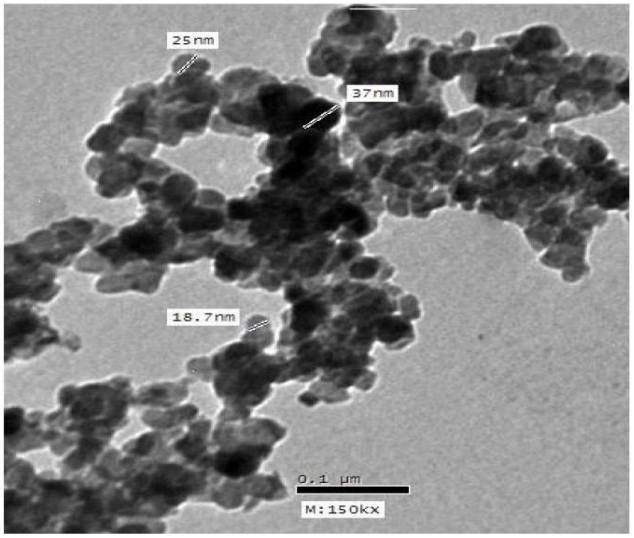

(b)

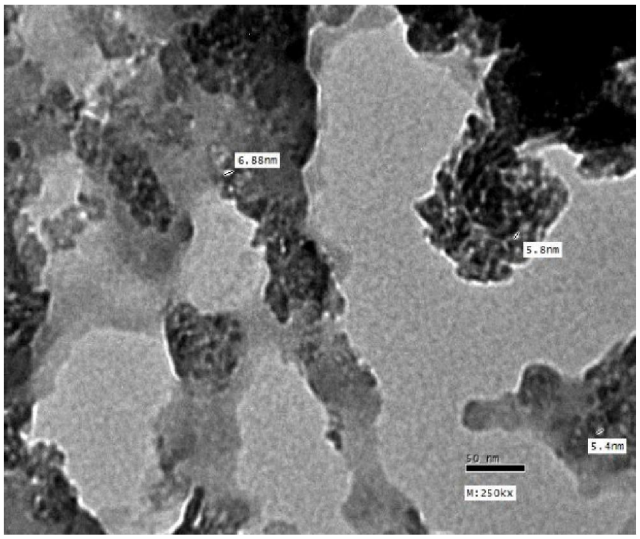

(d)

Figure 7 : TEM images of: NiMoS/Al_2O_3(a), NiMoS/TiO_2(b) NiMoS/Ti(50%)-Al_2O_3(c),and NiMoS/Ti(15%)-Al_2O_3(d)

or may be due to interference with the peaks of rich titania containing catalysts, or may be due to that the particles size is less than 5 nm[44]. These results suggest that, the TiO_2-Al_2O_3 composite support can weaken the strong interaction between the γ -Al_2O_3 support and NiMo(CoMo) oxides and sulfide phases. This is in accordance with the FTIR results. Titania can be sulfided as indicated by FTIR, and promote sulfidation[24] part of Ti^{3+} can be reoxidized easily, where, some particles occur[24,25].

The morphology, size and crystalline characterizations of the sulfided catalysts were observed by the TEM analysis performed over several areas on the TEM micrograph of the sulfided catalysts. A few TEM images of the sulfided samples are shown in Figure 7 It is known that MoS_2 presents layered phase with a hexagonal crystallographic structure. Indeed, the micrographs have their typical fingers. The edge sites of the edge-bonded MoS_2 clusters, which are perpendicular to the support surface, might have a lower metal-support interaction in comparison with the MoS_2 clusters basally bonded with the support. The NiMoS (CoMoS) phase could be formed mainly in the basal-bonded MoS_2 single layer(NiMo-S type I) and in the basal bonded MoS_2 multi-layer (NiMo-S type II)[48]. It is noteworthy that all samples possesses the nanoparticles of MoS_2 phase in the range 2-37 nm and the lowest MoS_2 crystal size were observed for alumina and Ti(15%)-Al supported catalysts(Figure7 a, d)The crystal size follows the

Full Paper

order $NiMo/TiO_2$> NiMo/Ti(50%)-Al > NiMo/Ti(15%)-Al≈NiMo /Al > CoMo/Ti(15%)-Al. Figure7a shows that alumina was a very fine powder, in good agreement with the powder XRD pattern of γ-Al_2O_3 which showing broad diffraction peaks(Figure 4). The micrograph of $NiMoS/Al_2O_3$ displays many dark dots with diameters ca. 4 nm. Although in many cases it becomes a difficult task to distinguish these blank dots of alumina from the dark images of sulfided NiMo crystallites in case of particle with sizes less than 3 nm, these dots may be represents the distribution of MoS_2 particles over the fine powder of alumina with less darkness, the microgram also show a distribution of a very narrow pores with a uniform pore size of alumina support which was confirmed by an N_2 isotherm analysis. Figure 7b represents the TEM microgram of $NiMoS/TiO_2$ catalyst, here a well ordered and repeated cubic morphology can be observed, the catalyst particles are with good distribution and large distances or holes can also be observed, also the dark dots which is considered to be of MoS_2 particles are large in size and are slightly agglomerated in some portions than those of $NiMoS/Al_2O_3$, but with sizes doesn't exceed 37 nm in maximum this can be due to the small surface area of titania support compared to that of alumina support. The TEM microgram of NiMoS/Ti(50)-Al catalyst is given in Figure 7c, we can note the distribution of the MoS_2 black dots over the transparent particles of Ti(50%)-Al support, these dots or spheres are in range of 10 nm thickness, also presence of pores between all the particles is obvious, the microgram in general closely resembles the microgram of $NiMoS/TiO_2$, but the particles here are more closed may be due to the presence of alumina particles between the TiO_2 particles. A representative TEM micrograph of sulfided NiMo/Ti(15%)-Al catalysts is shown in Figure 7d. The MoS_2 like structures are made up of small ordered sections which are often bent on a longer scale suggesting a strong interaction with the support surface in accordance with the FTIR Figure 1d. The fine alumina particles accumulated in small sections are apart with large distances or holes each other due to the introducing of titania with 15%, these holes could facilitate the penetration of target materials onto active sites in the inner surface for the applications of the catalytic reaction and the adsorption process.

In case of CoMoS/Ti(15%)-Al catalyst (Figure7e) a predominantly TiO_2 nanotubes with polyhedral morphology have been observed. The TiO_2 nanotubes in some cases had a central hollow open ended, and multiwall structure[49], here the tubes are of sickness size of 2 nm, the tubes are distributed parallel and perpendicular each other and we can note the very dark dots even of alumina or of MoS particles in small sections around them.

The formation of titania nanotubes here is of great importance and is a novel, since we prepared them at room temperature and with high concentration from the starting solution in the time as it is well known that most common method of preparation of titania nanotubes is the hydrothermal method which involves higher temperature (150 ºC) and pressure (use of autoclave).

The TEM micrographs of the sulfided TiO_2 and Ti (50%)-Al catalysts Figure7b, c clearly shows the edge planes of MoS_2 –like slabs oriented inline with or slightly tilted from the electron beam.

To evaluate the interaction between Ni (Co) and Mo species, catalysts containing only Ni(Co) or Mo,NiMo,andCoMo, were studied by H_2-TPR., Figure8(a-e) shows this study. Under the applied conditions, all the species can be reduced. Regarding the Ni supported on titania-containing samples, the presence of three reduction processes can be observed. These being associated with the presence of Ni^{2+} species in different environments. The high reduction temperatures(823 and 945ºC) related to that the reduction of the Ni^{+2} species occurs at higher temperatures,than that corresponding to the reduction of bulk NiO, which shows a single reduction peak at around 300ºC[50] suggesting that the reduction of Ni^{2+}, forming a phase different from NiO, and these Ni^{2+} ions strongly interact with the support and located inside the pores.

For Ni/Al_2O_3 the maximum reduction temperature is shown as a broad band centered around 870ºC with a shoulder around 700ºC. The broadness of this peak indicates the presence of more than one peak. These peaks indicate different reduction behavior

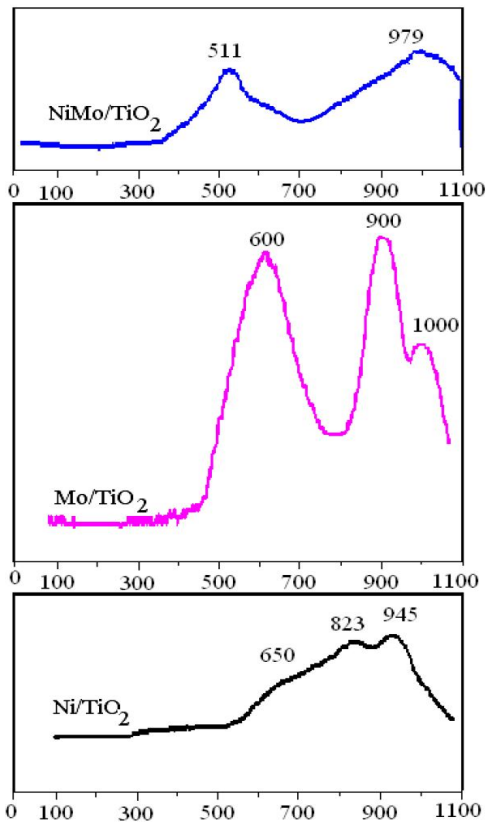
511
979
NiMo/TiO2
0 100 300 500 700 900 1100
600
900
1000
Mo/TiO2
0 100 300 500 700 900 1100
650
823
945
Ni/TiO2
0 100 300 500 700 900 1100

(a)

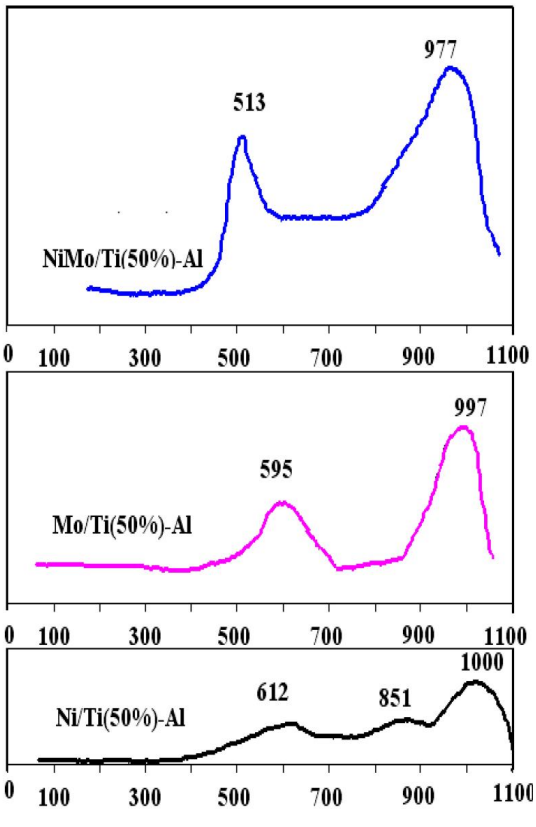
513
977
NiMo/Ti(50%)-Al
0 100 300 500 700 900 1100
595
997
Mo/Ti(50%)-Al
0 100 300 500 700 900 1100
612
851
1000
Ni/Ti(50%)-Al
0 100 300 500 700 900 1100

(b)

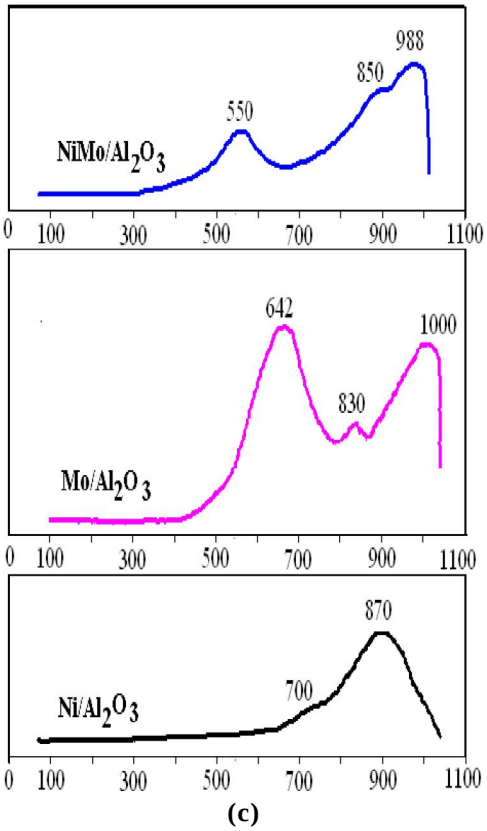
550
850
988
NiMo/Al2O3
0 100 300 500 700 900 1100
642
830
1000
Mo/Al2O3
0 100 300 500 700 900 1100
700
870
Ni/Al2O3
0 100 300 500 700 900 1100

(c)

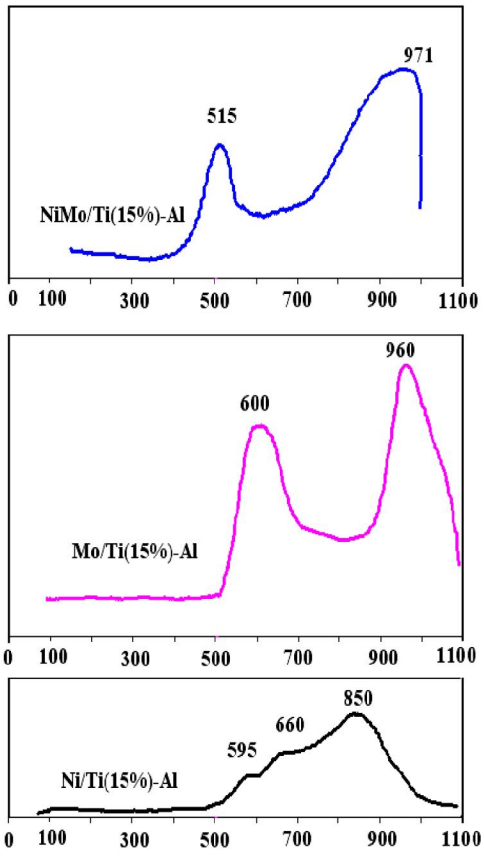
515
971
NiMo/Ti(15%)-Al
0 100 300 500 700 900 1100
600
960
Mo/Ti(15%)-Al
0 100 300 500 700 900 1100
595
660
850
Ni/Ti(15%)-Al
0 100 300 500 700 900 1100

(d)

Full Paper

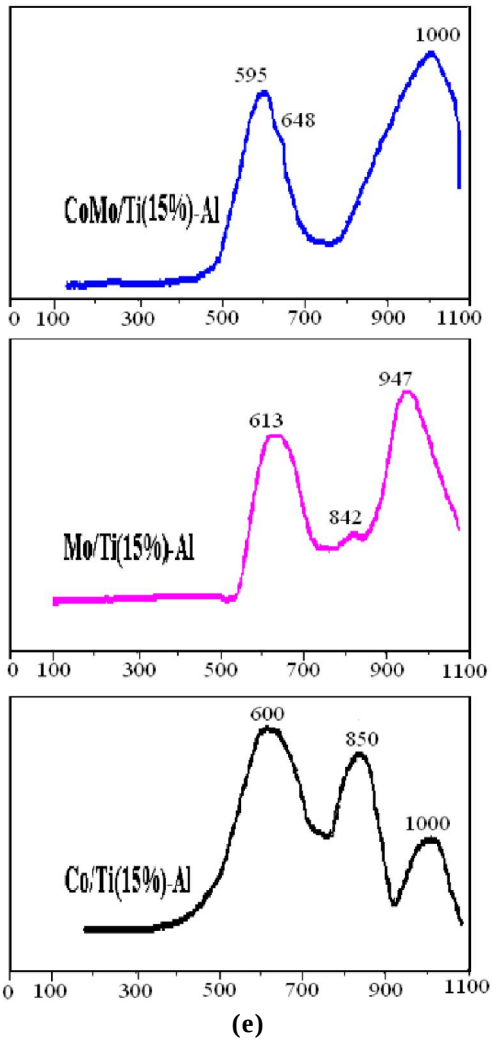

(e)

Figure 8 : TPR patterns of Ni, Mo, and NiMo supported on $TiO_{2\ (a)}$, $Al_2O_{3(b)}$. TiO_2(50%)-Al_2O_3(c), TiO_2(15%)-Al_2O_3(d) Co,Mo,andCoMo supported on TiO_2(15%)-$Al_2O_{3(e)}$

of Ni^{+2} species. For Mo supported catalysts, two main beaks and a shoulder were observed, with the exception of Mo/titania which shows three peaks. The low-temperature (around 600 ºC)peak can be assigned to the partial reduction (Mo^{6+}→Mo^{4+}) of amorphous highly reactive, multilayered Mo oxides or octahedral Mo species[45]. The high temperature peaks (947-1000 ºC) comprise the reduction of all Mo species, including highly dispersed tetrahedral Mo species. The shoulders may be due the intermediate-reducible crystalline phases of orthorhombic MoO_3 [51]. After the incorporation of Ni into Mo supported catalysts, the first reduction peak of the reactive Mo species is shifted to lower temperatures(from around 600 ºC to 515 ºC in case of NiMo/Ti (15%)-Al, to 511 ºC in case of NiMo/TiO_2, and to 513 ºC in case of NiMo/Ti(50%)-Al), indicating that the addition of Ni promoted the reducibility of Mo. This suggests that there was an interaction between Ni and Mo species. The lowest shift of the first peak of the active Mo species(octahedral form) was noticed in case of NiMo/Al_2O_3 (from around 600 ºC to 550 ºC), here it appears obviously that the incorporation of titania into alumina plays an important role on the reduction of Mo species[18]. Looking to all the TPR figures, the different peaks at different temperatures for different catalysts indicate how the composition of the support plays an important role on the loaded catalyst. A comparison of the TPR spectra of the Ni and Co supported onTi (15%)-Al (Figure8d, e) shows that nickel promotes the easy reduction of Mo species(specially the first peak of the reactive octahedral Mo) than cobalt, where they are reduced from around 600 ºC to 515 ºC in case of Ni supported on Ti(15%)-Al, while it has just reduced from 613 ºC to 595 ºC in case of Co supported on the same support. This may be reflect why Ni is more active than Co in many cases as a hydrodesulfurization catalyst. The change in the reducibility of Mo-Ni (Co) is due to the surface interaction between Ni(Co) and Mo. Therefore, it seems evident that the Ni-Mo-O or Co-Mo-O phase is the precursor of the Ni-Mo-S or Co-Mo-S phase known as the HDS active site[52].

Catalytic activity measurements

In this part, the HDS of GO was conducted by using different NiMo and CoMo supported catalysts prepared completely in the lab as discussed before.

The performance tests were monitored by changes in sulfur content. The HDS percentage was calculated as:

$$HDS\ \% = \left| \frac{S_{feed} - S_{product}}{S_{feed}} \right| X\,100$$

Where S_{feed} and $S_{product}$ indicate the concentration of sulfur in the feed and products, respectively[53,53]. In this section, we discuss the impact of the operating conditions, temperature, 320-400ºC, LHSV, 0.5-4h^{-1}, pressure and hydrogen to oil ratio constant at 6.0MPa, 450 v./v., respectively, on HDS processes.

Single stage operation

Effect of reaction temperature

The reaction temperature plays an important role in HDS. To study the influence of the reaction temperature on the HDS of gas oil feedstock, experiments using the prepared catalysts were conducted at 320, 360, and 400 ºC, respectively. As shown in Figures 9-11, it is obvious that the HDS increases rapidly with increasing reaction temperature. The HDS exceeds 99% and is close to 100% when the reaction temperature reaches 400 ºC High temperature favors the formation of vacancies on MoS_2 edge surfaces, which are the coordinative unsaturated molybdenum active sites located at the edge of MoS_2 [54]. It can be found that, the HDS efficiencies of the prepared catalysts reach a maximum value at titania content of 15%. The order of catalytic activities at all operating conditions for HDS is arranged as follows: NiMo/Ti(15%)-Al > NiMo/Ti(50%)-Al_2O_3 > NiMo/TiO_2 > NiMo /Al_2O_3 > CoMo/Ti(15%)-Al.

Previous- results and new evidence on the role of titania in supported HDS catalysts are analyzed in order to construct a rational explanation for the different findings in Ti-containing HDS catalysts. Some of the important findings is as follow; after sulfidation and in reaction conditions, where the catalyst is in the presence of a high hydrogen pressure, titania can be reduced and sulfided in part as indicated by FTIR. Moreover, under these conditions the reduced titania and titanium sulfide species, the latter having narrow gap semiconductor properties, will have nearly metal conductivities. Ti^{+3} species formed under HDS reaction conditions act as electron donors. These electrons can be easily transferred, through the conduction band of the support, and be injected to the Mo 3d conduction band. This causes a weakening of the Mo-S bonds and helps the creation of more coordinatively unsaturated sites (CUS). In other words, the anatase TiO_2 makes it easier to form octahedral coordination, which facilitates the formation of the CUS or sulfur vacancies that are favorable for HDS reaction[55]. Characterization results of H_2-TPR verify that the incorporation of TiO_2 into Al_2O_3 support can adjust the interaction of support and active metal, and thus improve the reducibility of molybdenum on TiO_2 containing catalysts. In the case of rich titania supports (Figure 8) part of Ti^{+3} ions can be oxidize easily, where some segregation of TiO_2 particles occurs[24].

From Figures 9-11, the activities of NiMo catalysts containing titania are all higher than that of the Al_2O_3-supported catalyst. Characterization results of H_2-TPR and FTIR verify that, the TiO_2-Al_2O_3 composite support obtained by dispersing TiO_2 through the surface of γ-Al_2O_3 can weaken the interaction between γ-Al_2O_3 and molybdenum oxide and thus decrease the amount of four-complexing Al^{+3} ions, thus effectively improving the sulfidation of the active species[47], consequently improving the activity of the catalyst This support still keeps a larger sur-

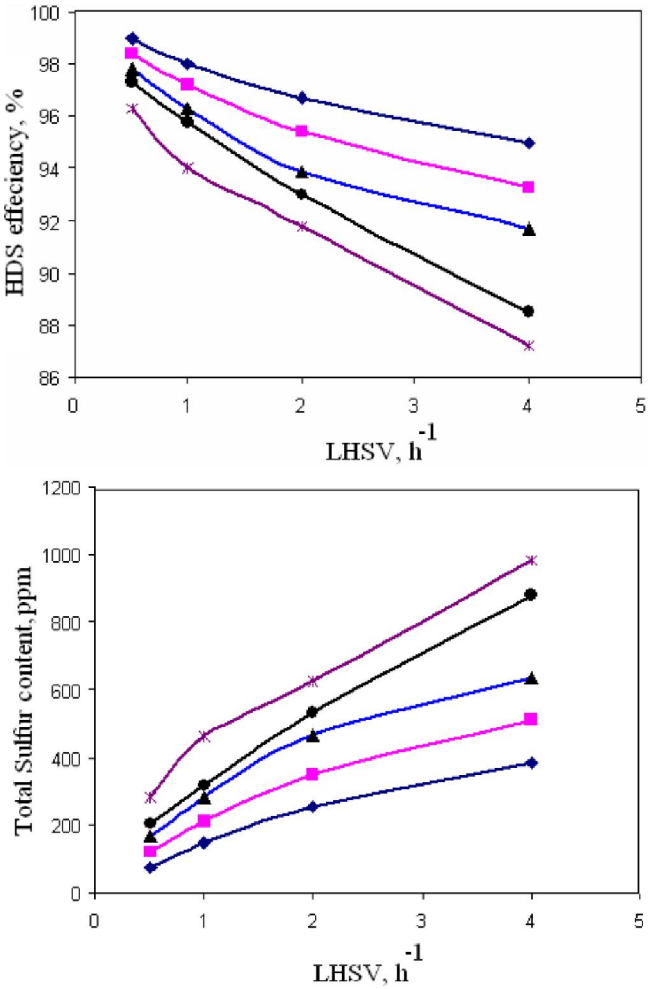

Figure 9 : Sulfur removal and total sulfur content of gas oil products as a function of LHSV. (Temperature: 320 ºC, Pressure:6MPa, H_2/oil ratio:450 v./v.) (♦)NiMo/Ti(■)-Al, (%)NiMo/Ti(50%)-Al,(▲)NiMo/TiO_2, (•)NiMo/Al_2O_3 (*)CoMo/Ti(15%)-Al

Full Paper

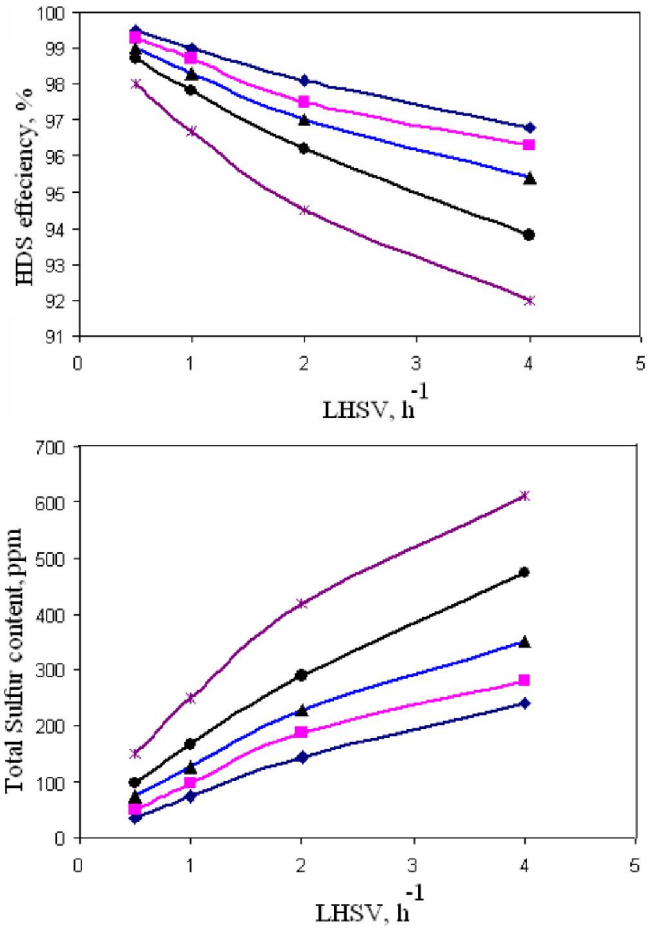

Figure 10 : Sulfur removal and total sulfur content of gas oil products as a function of LHSV. (Temperature: 360 °C, Pressure:6MPa, H_2/oil ratio:450 v./v.) (♦)NiMo/Ti(15%)-Al, (■)NiMo/Ti(50%)-Al,(▲)NiMo/TiO_2, (•)NiMo/Al_2O_3 (*)CoMo/Ti(15%)-Al

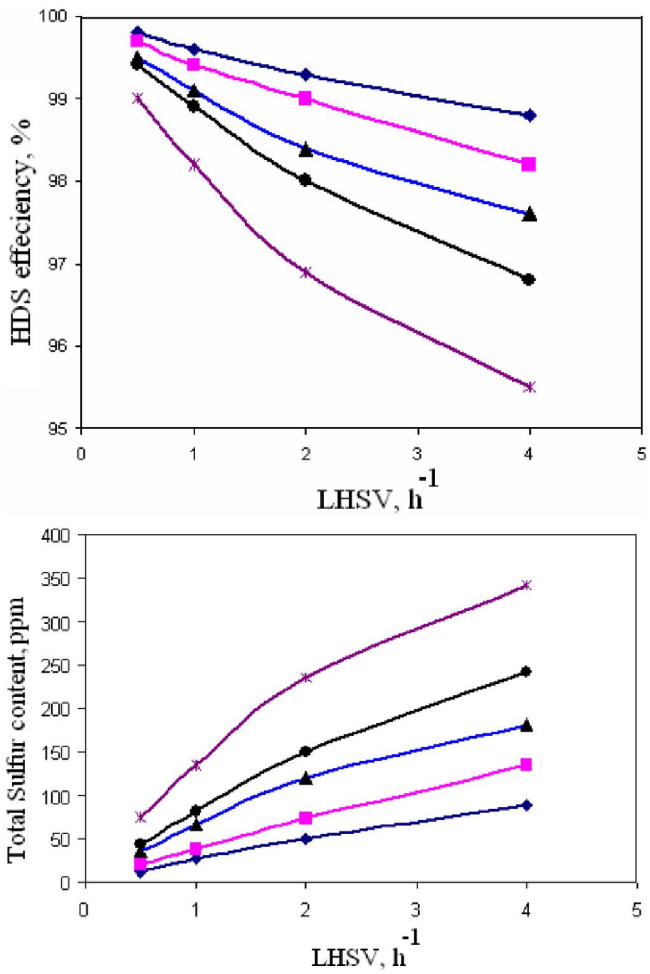

Figure 11 : Sulfur removal and total sulfur content of gas oil products as a function of LHSV(Temperature: 400 °C, Pressure:6MPa, H_2/oil ratio:450 v./v.) (♦)NiMo/Ti(15%)-Al, (■)NiMo/Ti(50%)-Al, (▲)NiMo/TiO_2, (•)NiMo/Al_2O_3 (*)CoMo/Ti(15%)-Al

face area and suitable pore structure in comparison to the pure Al_2O_3 support. The results reported here indicate that adequate design of the characteristics of the catalytic support is of great importance in the development of better HDS catalysts.

The low activity of pure titania supported catalyst is due to its lower surface are Figures 9-11clearly show that, the NiMo/Ti(15%)-Al catalyst is superior for gas oil HDS compared with CoMo/Ti(15%)-Al catalyst, since it gives lower concentration of sulfur in the product. This behavior can be attributed to the different reaction mechanism followed during gas oil HDS (hydrogenolysis and hydrogenation) and also to the several compounds exhibiting different reactivities that are being converted[53]. TPR spectra of the Ni (Figure 8a) and Co(Figure 8e)catalysts supported on Ti(15%)-Al showed that Ni promotes the easy reduction of Mo species compared with Co. It has been found that Co facilitated the interaction with the support at the same composition than Ni as indicated by Jie et.al[57].The incorporation of Ni or Co to MoS_2 structure can significantly changes the active sites on MoS_2.. It is generally accepted that unsaturated sulfur vacancies increase in the Ni promoted catalyst than Co promoted one[54].

Effect of LHSV

The LHSV is the ratio of the feed volumetric flow rate to the catalyst volume. It gives a measure of how much time lapses while the reactant interact with the catalyst active sites. A reduction in the flow rate could allow more time for conversion. As a result, refiners are able to predict how much catalyst

will be needed to achieve a certain amount of conversion. A through study of the relationship between LHSV and HDS conversion of GO, would contribute much to the optimization of HDS process

Figures 9-11 show the conversion of sulfur compounds against the LHSV value. The LHSV value was varied from 0.5 to 4 $h^{-1}$with varying the temperature from 320 to 400 ºC, the pressure and H_2/ oil ratio were maintained constant at 6.0 MPa and 450 v./v., respectively. The conversion of sulfur compounds decrease as the LHSV value increases. which means that, as the LHSV value increased, the reaction time decreased and conversion was reduced. Figure11 shows a higher increase in HDS of GO from LHSV values of 1 to.5 h^{-1}. This may be due to the combined effect of high severity, in terms of both temperature and LHSV. After 1h^{-1} LHSV, the conversion decreases considerably to reach about 95.5 % at 4 h^{-1}. This is because the residence time of GO is shortened on the catalyst with the LHSV increasing. When the LHSV was 0.5 h^{-1}, the sulfur removal reached 99.8 %. Therefore, the suitable LHSV was 0.5 h^{-1} under this experimental conditions.

By looking through Figures 9-11 we can note and conclude that; NiMo/Ti(15%)-Al catalyst has the better catalytic activity towards the HDS of GO in the single stage operation, since the S% is reduced from 74 ppm to 12 at 0.5 h^{-1} LHSV by increasing the temperature from 320 to 400 ºC. NiMo/Ti(50%)-Al catalyst coming after NiMo/Ti(15%)-Al, where the S% is reduced from 120 to 20 ppm at the same operating conditions. NiMo/TiO_2 catalyst has a better HDS catalytic activity than NiMo/Al_2O_3 catalyst where the S% is reduced from 166 to 35 ppm in case of NiMo/TiO_2 and from 204 to 43 ppm in case of NiMo/Al_2O_3 catalyst. Although TiO_2 support has a less surface area (72 m^2g^{-1}) than Al_2O_3 (247 m^2g^{-1}), the cause is as mentioned before in the section of TPR, the active octahedral Mo species have a lower reduction temperature peak in case of titania support (600ºC)(Figure 8c) than that in case of alumina support(642ºC) (Figure 8d), and the incorporation of Ni to Mo in case of titania lowered this active peak to 511ºC than that in case of alumina 550 ºC

CoMo/Ti(15%)-Al catalyst has the lowest HDS catalytic activity, since the S% is reduced from 281 to 75 ppm at the maximum operating conditions (T = 400 ºC and LHSV = 0.5 h^{-1}). The lowest HDS activity of CoMo/Ti(15%)-Al catalyst than NiMo/Ti(15%)-Al catalyst is as just above mentioned, that Co facilitate the interaction of the Mo species to the support so reducing their reduction and of therefore their overall reactivity.

These results show that, the sulfur content is still above the goal of this study i.e. above 10 ppm which is the world demand nowadays, so we had to apply the dual bed operation as will be discussed later.

Dual catalytic bed system

The real task of the present study is how to reduce the sulfur species in the gas oil to be less than 15ppm. Modern ultra-low- sulfur diesel (ULSD) units use a combination of CoMo and /or NiMo catalysts that are operated under sever conditions to hydroge-

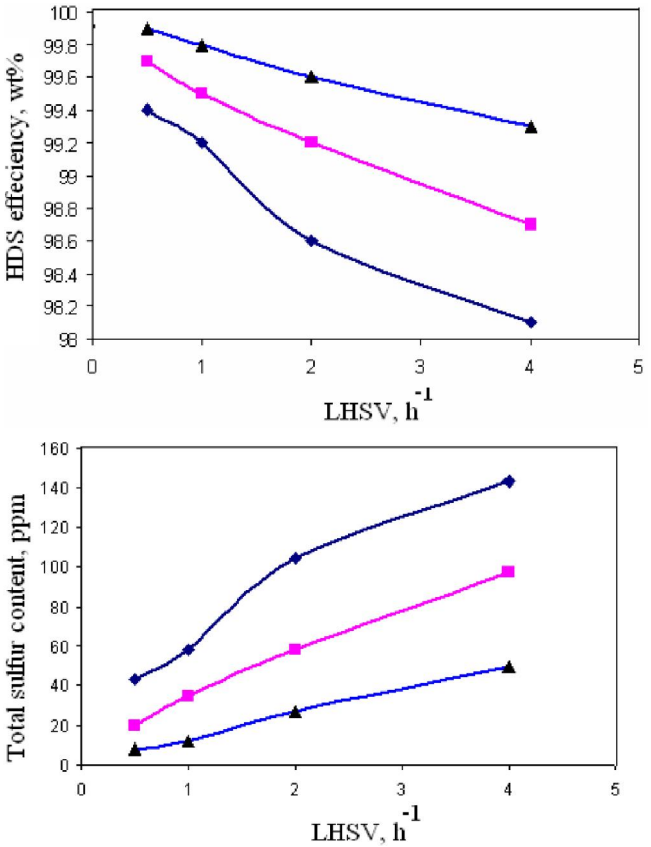

Figure 12 : Sulfur removal and total sulfur content of gas oil products as a function of LHSV by using CoMo/NiMo double layered bed (▲) Temperature: 320°C (■)Temperature: 360°C (♦)Temperature: 400°C (Pressure:6MPa, H_2/oil ratio: 450v./v.)

nate the sterically hindered organic sulfur compounds by staged and layered catalysts beds. The first stage and / or-layer aims to desulfurize completely the reactive sulfur species by direct desulfurization rout and additionally refractory sulfur species by hydrogenation route on CoMo as much as possible. Where the inhibition of co-present species of the feed gas oil must be moderated by selecting the catalysts as well as the reaction conditions. NiMo being superior in the practical desulfurization and suffers much less inhibitions than CoMo supported catalyst.

In the present study, the catalyst system consists of both CoMo/Ti(15%)-Al and NiMo/Ti(15%)-Al in special arrangement depends upon two-layer catalyst beds, CoMo catalyst is the upper layer and NiMo is the lower layer. The ratio of the catalyst types is 1:1. The two-layer catalyst beds with the best HDS support of respective layers under respective conditions of 320-400 ºC, 0.5-4h^{-1}, 6.0 MPa and 450 v./v. can be a logical approach to achieve deep HDS of GO The experimental resultes revealed that it is possible to achieve higher levels of HDS efficiency by using CoMo/NiMo layers process compared to NiMo/Ti(15%)-Al in a single layer process. However, high temperatures or low space velocities are also needed with this catalyst system to obtain reasonable levels of sulfur reduction. The result data from Figure12 shows how the two- layer operation led to the reduction of sulfur content in the feed (7600 ppm) to 8 ppm at maximum operating conditions (T = 400 ºC and LHSV = 0.5 h^{-1}) concluding that, by a simple modified method of catalyst preparation in the nanoscale and by the dual stage application, we were successful to reduce sulfur present in the gas oil to 8 ppm which matches the world demand. The obtained product can meet the sulfur regulations of Euro IV specification of ultra clean diesel fuel.

CONCLUSION

Based on the characteristics of the supports and catalysts determined in this investigation and also on the performance of the investigated catalysts, the following conclusion can be raised:

- High specific surface area mixed oxide support can be prepared using delayed co-precipitation of TiO_2 with alumina. The N_2 adsorption of NiMo(CoMo) supported catalysts indicates that the added NiMo (CoMo) particles entered inside the pores of the support.
- The XRD results indicated that the active metal oxides and sulfides are present as amorphose nanoparticles.
- The TEM micrographs of the sulfide catalysts clearly show the edge planes of MoS_2-like slabs oriented in line with or slightly tilted from the electron beam.
- FTIR results verify that the modification of the surface of alumina with TiO_2 eliminates the most of reactive surface hydroxyl groups and avoids the formation of tetrahedral Mo oxide species, resulting in an increase of octahedral Mo active species, which facilitates the formation of the coordinative unsaturated sites or sulfur vacancies that are favorable for HDS reaction. Titanium species formed during sulfidation act as promoter of the Mo phase giving rise to a synergy effect. This synergy effect seems to be related to the electronic properties of the sulfide TiO_2 surface.
- The TPR profiles indicate the two step reduction characteristics of Mo^{6+} to lower oxidation state such as Mo^{4+} and Mo^0. The incorporation of TiO_2 into Al_2O_3 support can adjust the interaction of support and active metal, and thus improve the reducibility of molybdenum on TiO_2-Al_2O_3 support.
- TPR spectra of the Co and Ni promoter catalysts showed that Ni promotes the easy reduction of Mo species compared with Co.
- The HDS efficiency reaches a maximum at NiMo/TiO_2-Al_2O_3 catalyst with Ti content of 15%, which is consistent with its higher reducibility and the higher CUS proportion.
- NiMo catalyst was found to be superior to CoMo catalyst for gas oil HDS.
- Dual layer catalyst bed can be a logical approach to achieve ultra deep HDS of diesel fuel at acceptable reaction conditions.
- The optimal HDS product can meet the sulfur regulation of Euro IV specification of ultra clean diesel.

REFERENCES

[1] E.Hong, L.Jianmei, W.Hai; Appl.Catal.B Environ.,**165**, 269 **(2015)**.
[2] W.Danhong, L.Ni, Z.Jianyong, Z.Xin, Z.Wenhao, Z.Minghui; J.of Molecular Catal., **393**, 47 **(2014)**.
[3] Y.Yanjiao, X.Jin, L.Wang, Q.Zhang, G.Xiong, C.Liang; Catalysis Today, **175,** 460 **(2011)**.
[4] X.Li, a.Wang, m.Egorova, r.Prins; J.Catal., **250**, 283 **(2005)**.
[5] N.Kunisada, K.H.Choi, Y.Korai, I.Mochida, K.Nakano; Appl.Catal.A, **279**, 235 **(2005)**.
[6] K.Jaroszewska, M.Lewandowski, J.R.Grzechowiak, B.Szyja; Catalysis Today, **176**, 202 **(2011)**.
[7] J.Park, K.Nakano, Y.Kim, J.Miyawaki, S.Yoon, I.Mochida; Catalysis Today, **164**, 100 **(2011)**.
[8] D.Valencia, T.Klimova; Catalysis Today **166**, 91 **(2011)**.
[9] R.Fereshteh, S.Takehito, M.R.Ali, N.K.Ali, J.J.Kheirollah; J.of Catal., **299**, 321 **(2013)**.
[10] L.Weikun,S.Wenjin, P.Liqing, W.Zhongfang, Z.Nan, L.Juanjuan, Z.Jinbao, Y.Xaodong, F.Weiping; J of Catal., **303**, 80 **(2013)**.
[11] K.Taegon,A.A.Syed, A.Khalid, P.Joo-II,Y.Mohmmed, H.Y.Seon, M.Isao; J of Indust.and Engen.Chem., **19**, 1527 **(2013)**.
[12] P.Castillo-Villalon, J.Ramirez, J.A.Vargas-Luuciano; J of Catal., **320**, 127 **(2014)**.
[13] P.E.Boahene, K.Soni, A.K.Dalai, J.Adjaye; Applied Catalysis B: Environmental, **101**, 294 **(2011)**.
[14] Y.Zhao, M.Xue, M.Cao, J.Shen; Applied Catalysis B: Environmental, **104**, 229 **(2011)**.
[15] K.C.Mouli, K.Soni, A.Dalai, J.Adjaye; Applied Catalysis A, **404**, 21 **(2011)**.
[16] A.Duan, G.Wan, Y.Zhang, Z.Zhao, G.Jiang, J.Liu; Catalysis Today, **175**, 485 **(2011)**.
[17] J.N.Diaz De Leon, T.A.Zepedo, A.G.Nunez, D.H.Galvan, S.Funetes; J.of Catal., **321**, 51 **(2015)**.
[18] S.A.Hanafi, M.S.Mohamed; Energy Source, Part A, **33**, 495 **(2011)**.
[19] A.H.Samia, M.S.Elmelawy, H.A.El Syed, E.S.A.Sultan *"petroleum science and technology"Journal*, **27**, 83 **(2009)**.
[20] A.H.Samia, S.M.Elmelawy; *"petroleum science and technology"Journal*, **26**, 1005 **(2008)**.
[21] A.H.Samia, H.A.El-Sayed, M.S.El melawy, A.S.El-Sayed; *Energy sources, part A*, **31**, 831 **(2009)**.
[22] A.H.Samia; "*Petroleum Science and Technology"* Journal, **25**, 1247 **(2007)**.
[23] M.G.Eskaroz; Hydroc.Proc., **87(2)**, 103 **(2008)**.
[24] W.Huang, A.Duan, Z.Zhao, G.Wan, G.Jiang, T.Dou,K.H.Chung, J.Liu; J.Catal.Today, **131**, 314 **(2008)**.
[25] Choi, Ki-H, Y.Korai, I.Mochida; Appl.Catal.A, **260**, 229 **(2004)**.
[26] I.D.Gonza Lez,R.M.Navarro, A.M.C.Ivarez-Galvan, F.Rosa, J.L.G.Fierro; Catal.Comm., **9**, 1759 **(2008)**.
[27] J.Erena, I.Sierra, M.Olazar, G.Gayubo, A.T.Aguayo; Ind.Eng.Chem.Res., **47**, 2238 **(2008)**.
[28] C.Ma,Y.Chang,W.Ye, W.Shang, C.Wang; J.Colloid and Interface Sci., **317**, 148 **(2008)**.
[29] R.John, K.D.Abhaya, G.S.Allen; J.Catal., **173**, 145 **(1998)**.
[30] F.Cavani, F.Trifiro, A.Vaccari; Catal.Today. **11**, 173 **(1991)**.
[31] S.A.Hanafi, H.A.EL-Sayed, M.S.Elmelawy, E.S.A.Sultan; Petrol.Sci.and Technol., **27**, 83 **(2009)**.
[32] M.V.Landau, E.Dafa, M.L.Kaliya, T.Sen, M.Herskowitz; Microporous and Mesoporous Mat., **49**, 65 **(2001)**.
[33] B.Demirel, S.Fang, E.N.Gives; Appl.Catal.A, **201**, 177 **(2000)**.
[34] Y.Araki, K.Honna, H.Shimada; J.Catal., **207**, 361 **(2002)**.
[35] A.A.Cecilio, S.H.Pulcinell, C.V.Hamtilli; Sol-Gel.Sci.Techno., **31**, 87 **(2004)**.
[36] J.Ramirez, L.Cedenol, G.Busca; J.Catal., **184**, 59 **(1999)**.
[37] J.A.Van Veen, H.A.Colijn, P.A.J.M.Hendriks, A.J.Van Welsens; Fuel Proc.Technol., **35**, 137 **(1993)**.
[38] Eijbouts; Appl.Catal.A., **158**, 53 **(1997)**.
[39] X.Chen, Y.Dong, Zhao, C.Zhao, T.Zhao; Energy&Fuels, **22**, 3571 **(2008)**.
[40] JCPDS Powder Diffraction File, International Center for Diffraction Data, Swarthmore, PA, **(1989)**.
[41] S.Y.Jung, S.J.Lee, JeParak, S.Lee, H.K.Jun, T.J.Lee; Ind.End.Chem.Res., **47**, 4909 **(2008)**.
[42] G.Wan, A.Duan, Z.Zhao, G.Jiang, D.Zhang, Li, T.Uou, K.H.Change; Energy & Fuels, **23**, 81 **(2009)**.
[43] C.Leyva, J.Ancheyta, M.S.Ranas, G.Marroguin; Fuel, **86**, 1232 **(2007)**.
[44] B.Morteza, M.H.Sayed; Ind.Eng.Chem.Res., **48**, 3331 **(2009)**.
[45] D.Tichit, M.Lhouty, A.Guida, B.Chiche, F.Figueras, A.Autoroux, D.Bartalini, E.Garrone; J.Catal., **151**, 50 **(1995)**.
[46] L.Gouran, L.Wei, Z.Minghui, T.Keyi; Catal.Today, **93-95**, 595 **(2004)**.

Full Paper

[47] S.M.Lia, L.M.Gan, L.H.Lia, W.D.Zhang, H.C.Zeng; J.Chem.Mater., **14**, 1391 **(2002)**.
[48] B.Pawelec, P.Castano, T.A.Zepeda; Appl.Surface Science, **254**, 4092 **(2008)**.
[49] A.Zoltan, M.Karoly, S.Agnes, A.Tundle, D.Kata, Andras, D.S.Pal; J.Appl.Catal.A, **340**, 153 **(2008)**.
[50] R.Hernadez – Huesca, J.Merida – Robles, A.Maireles- Lopez; J.Catal., **203**, 122 **(2001)**.
[51] S.Rajagopal, H.J.Marini, J.A.Marzari, R.Miranda; J.Catal., **147**, 417 **(1994)**.
[52] J.A.Marzari, S.Rajagopal, R.Miranda; J.Catal., **156**, 255 **(1995)**.
[53] S.K.Maity, J.Ancheyta, L.Soberanis, F.Alonso; Appl.Catal.A, **250**, 231 **(2003)**.
[54] M.Sun, J.Adjaue, A.E.Nelson; Appl.Catal.A, **263**, 131 **(2004)**.
[55] J.Ramirez, G.Macias, L.Cedeno, A.Gutierrez – Alejandr, R.Cuevas, P.Castillo; Catal.Today, **981(1-2)**, 19 **(2004)**.